Polarization of Photoluminescence from Partial Dislocations in 4H-SiC

Rii Hirano[1,2], Hidekazu Tsuchida[3], Michio Tajima[1*], Kohei M. Itoh[2], and Koji Maeda[4]

[1] Institute of Space and Astronautical Science/JAXA, Sagamihara 252-5210, Japan

[2] School of Fundamental Science and Technology, Keio University, Yokohama 223-8522, Japan

[3] Central Research Institute of Electric Power Industry, Yokosuka, Kanagawa 240-0196, Japan

[4] Department of Applied Physics, The University of Tokyo, Bunkyo, Tokyo 113-8656, Japan

E-mail: tajima@isas.jaxa.jp

Polarization characteristics of luminescence from partial dislocations (PDs) in 4H-SiC have been investigated by room-temperature photoluminescence (PL) imaging. The PLs from mobile PDs under optical excitation, which are 30°-Si(g) PDs, and PDs tilted by 6° from their Burgers vector (6°-PDs) were found to be polarized perpendicular to their dislocation lines. In contrast, the PL from immobile 30°-C(g) PDs was not polarized. The present results suggest that the carriers bound to the 30°-Si(g) and 6°-PDs have anisotropic wave functions and those bound to 30°-C(g) PDs have isotropic wave functions. © 2013 The Japan Society of Applied Physics

4H-SiC is a promising semiconductor material for highly efficient power devices and expected to be applicable for high voltage use, particularly in bipolar power devices. Under forward biasing of the diodes, however, the increased forward voltage drop that is caused by the anomalous expansion of Shockley stacking faults (SSFs) has been a serious issue in 4H-SiC bipolar power devices.[1,2] The expansion of these SSFs is achieved by the glide of partial dislocations (PDs) bounding the SSFs. Perfect dislocations in 4H-SiC with a Burgers vector of $1/3\langle 11\bar{2}0 \rangle$ are dissociated, following $1/3\langle 11\bar{2}0 \rangle \rightarrow 1/3\langle 10\bar{1}0 \rangle + 1/3\langle 01\bar{1}0 \rangle$,[3] into two PDs separated by an SSF. The dissociated PD with a silicon core [30°-Si(g)] glides in the direction of stacking fault expansion under forward biasing, while the counter PD with a carbon core [30°-C(g)] stays immobile.[4,5] We previously reported an experimental fact that suggested that the optically stimulated glide of 30°-Si(g) PDs was induced by the photoionization of electronic bandgap centers associated with the PDs.[6] It is known that the luminescence from 30°-Si(g) and 30°-C(g) PDs is observed at around 1.8[7–9] and 1.46 eV,[10] respectively. The dislocation-related luminescence, however, has not yet been confirmed to be intrinsic, having its origin in the energy levels associated with the PDs.

The symmetry of luminescence provides useful information on the elucidation of its origin. Polarized dislocation-related luminescence has been observed in many materials such as Si,[11] GaAs,[12] and diamond.[13,14] The recent progress of highly spatially resolved photoluminescence (PL) imaging[10,15,16] enables us to investigate the polarization of luminescence from individual PDs in 4H-SiC, which are separated enough to be resolved by the PL imaging technique.

In this study, the polarization of the PL from the PDs bounding the SSFs, which had been intentionally expanded in advance by scanning the sample with a laser beam at a high excitation intensity, was examined by PL imaging under a low excitation intensity. The results showed that PLs from 30°-Si(g) and anomalous PDs tilted clockwise by 6° from the Peierls potential valley of screw dislocations (6°-PDs) are polarized perpendicularly to their dislocation lines, while PL from 30°-C(g) PDs is not polarized.

A nitrogen-doped homoepitaxial layer of 70 μm thickness was grown on a 4H-SiC substrate offcut 8° towards [11$\bar{2}$0]. The nitrogen concentration in the epitaxial layer

was $\sim 10^{14}$ cm^{-3}. SSFs were expanded from grown-in basal plane dislocations or from dislocation sources introduced by indenting the sample surface with a microhardness stylus.

Room-temperature PL mapping experiments[17] using a focused laser beam as a scanning excitation source were performed to expand SSFs and simultaneously obtain their PL map images. For this purpose, an Ar-ion laser beam consisting of 364 nm lines focused down to a spot of ~ 2 μm diameter by using an objective (18×) was used to illuminate the sample surface at a high intensity of 5.4×10^4 W/cm^2, which allowed intentional expansion of SSFs. SSF-related emission selected by a band-pass filter transmitting light in the range of 2.95 ± 0.10 eV was detected by a photomultiplier (Hamamatsu Photonics R379).

Room-temperature PL imaging experiments using a cooled CCD camera (Princeton Instruments PIXIS:1024BR) were performed to observe the PL images of PDs. To observe 30°-Si(g) and 6°-PDs, four light-emitting diodes were used as the excitation sources with a peak wavelength of 365 nm and a low intensity of 0.1 W/cm^2. Since the luminescence from the 30°-C(g) PDs and the SSFs was weak, an Ar-ion laser, the same as that used for PL mapping, was employed for their observations with the excitation intensity of 4.7 W/cm^2. The monochromatic PL images were acquired through band-pass filters passing light of 1.64 ± 0.05 eV for 30°-Si(g) and 6°-PDs, light of 1.34 ± 0.03 eV for 30°-C(g) PDs, and light of 2.95 ± 0.10 eV for SSFs. For polarization analysis, a polarizer was inserted between the sample and the band-pass filters.

Figures 1(a) and 1(b) show two successive PL maps obtained under a high excitation intensity of 5.4×10^4 W/cm^2. The morphological features of the expanded SSFs are similar to those of previously reported triangular, trapezoidal, and rhombic SSFs, which are formed by the glide of 30°-Si(g) PDs dissociated from grown-in basal plane dislocations and basal dislocation sources near the surface.[18] Therefore, the two SSFs on the right side and the one on the left side in Figs. 1(a) and 1(b) are considered to have been expanded from grown-in basal plane dislocations and from basal plane dislocation loops introduced by the microhardness stylus, respectively. The inferred Burgers vectors are indicated schematically in Fig. 1(c). The PD segments bounding the SSFs, except for one marked, are almost parallel to the $\langle 11\bar{2}0 \rangle$ directions as reported previously,[19,20]

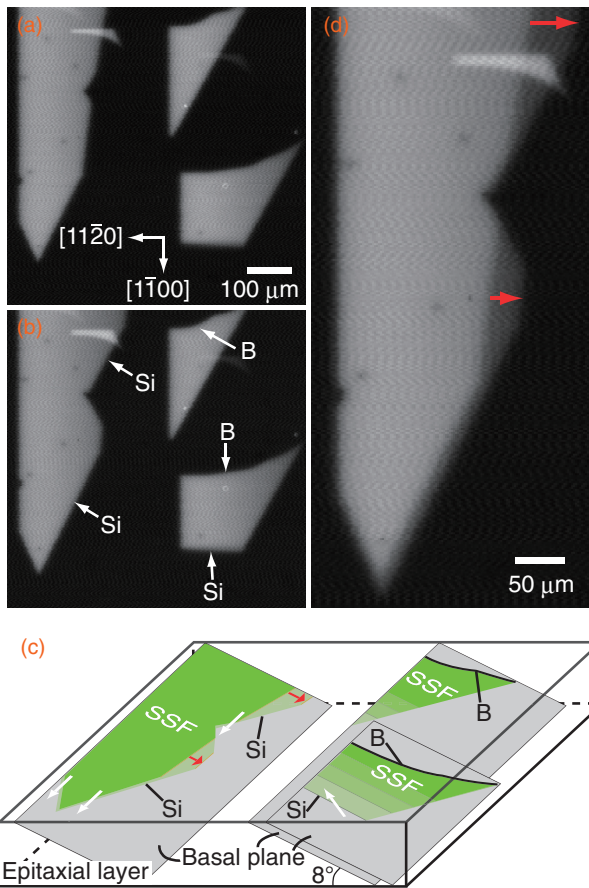**Fig. 1.** PL maps of SFFs obtained under excitation intensity of 5.4×10^4 W/cm² after (a) 1st and (b) 2nd scans. (c) Illustration of expanded SSFs in (a) and (b). White arrows indicate inferred Burgers vectors of the 30°-Si(g) PDs expanding the respective SSFs. The difference between (a) and (b) is shown in (d), an overlapped image of (a) and (b). Red arrows in (c) and (d) indicate the advance direction and distance of the SSF expansion toward [$\bar{1}\bar{1}20$]. Symbols of Si and B respectively indicate 30°-Si(g) PDs and grown-in basal plane dislocations from which the triangular SSFs were expanded. The indentation-induced basal dislocation loop from which the SSF was expanded is located outside the images.

Fig. 2. PL images acquired with band-pass filters (a) at 1.64 ± 0.05 eV for 30°-Si(g) and 6°-PDs, (b) at 1.34 ± 0.03 eV for 30°-C(g) PDs, and (c) at 2.95 ± 0.10 eV for SSFs. (d) Magnified image of the area in (b) framed in red. The 30°-C(g) PD segment encircled in blue demonstrates the interrupted PL intensity along the PD line. Symbols of Si and C indicate 30°-Si(g) PDs and 30°-C(g) PDs, respectively.

but the marked PD is obviously tilted by 6° from the direction of the Burgers vector or the Peierls potential valley of screw dislocations. Similar 6°-PD segments were reported to be observed when SSFs contracted under low excitation intensities[21] and they expanded under electron radiation.[22] Compared with 30°-Si(g) PD segments that advanced only a little from (a) to (b), the 6°-PD segment glided significantly to expand the SSF as shown in Fig. 1(d). The 30°-Si(g) and 6°-PDs bound the same SSF that exhibits a uniform PL intensity, which indicates that the driving force for SSF expansion or the glide of PDs arising from the electronic reduction of effective formation energy of SSF[6] was the same for the 30°-Si(g) and 6°-PDs. Therefore, the optical enhancement rate of 6°-PD glides is greater than that of 30°-Si(g) PD glides.

PL images of PDs and SSFs recorded after the image of Fig. 1(b) was acquired in the same area are shown in Figs. 2(a)–2(c) and magnified image of the Fig. 2(b) is shown in Fig. 2(d). Luminescent 30°-Si(g) PDs and 6°-PDs were observed in the monochromatic PL image in Fig. 2(a) obtained by using a band-pass filter for a photon energy range of 1.64 ± 0.05 eV. One might notice that the 6°-PD
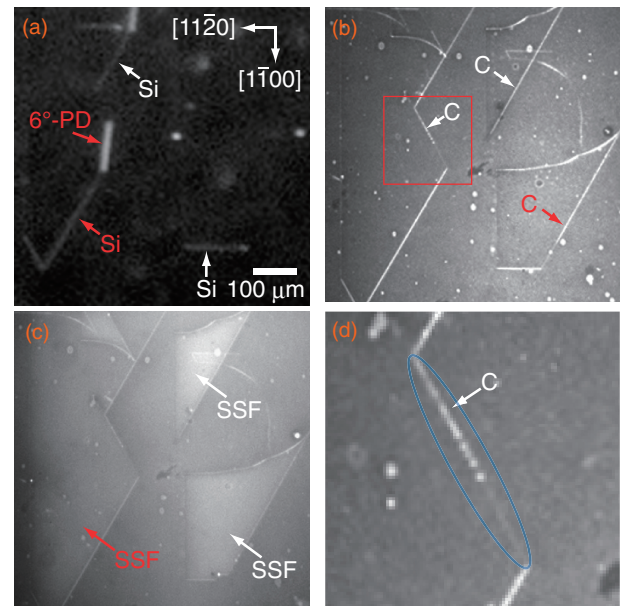
segment in Fig. 2(a) is slightly longer than that in Fig. 1(b). This is due to a slight expansion of the SSF during PL imaging to acquire Fig. 2(a) under a low excitation intensity. The intensity of the luminescence from 6°-PDs is approximately 5 times higher than that from 30°-Si(g) PDs. The monochromatic PL images from 30°-C(g) PDs shown in Fig. 2(b) could be observed only when the excitation intensity was so strong that the 6°-PDs glided out quickly, leaving less mobile 30°-Si(g) PDs and immobile 30°-C(g) PDs. The monochromatic PL image of SSFs shown in Fig. 2(c) was recorded after the image in Fig. 2(b) was acquired.

To elucidate the origin of the luminescence from 30°-Si(g), 30-°C(g), and 6°-PDs, the polarization of the PL marked by red arrows in Figs. 2(a)–2(c) was investigated. The polarization of the PL from the 30°-Si(g) and 6°-PDs was analyzed before acquiring the PL images in Figs. 2(b) and 2(c). Figure 3 shows that the PL from the 30°-Si(g) and 6°-PDs was distinctly polarized perpendicularly to the dislocation lines. We confirmed that this polarization feature was reproducible for other PDs of the same type and did not change under more intense excitation by Ar-ion laser illumination. The present result is consistent with the idea that the PL from 30°-Si(g) and 6°-PDs originates from the anisotropic nature of line defects. Polarized luminescence from dislocations was reported also in elementary diamond[13,14] and Si[11,16] where the polarization, however, is commonly parallel to the dislocation lines, which is a distinct difference from the present feature in 4H-SiC. A model considering the anisotropic effective mass of holes attempted to explain the polarization of luminescence from dislocations,[23] but it concluded that the polarization must be parallel to their Burgers vector, in disagreement with the polarization direction in the present results. The present
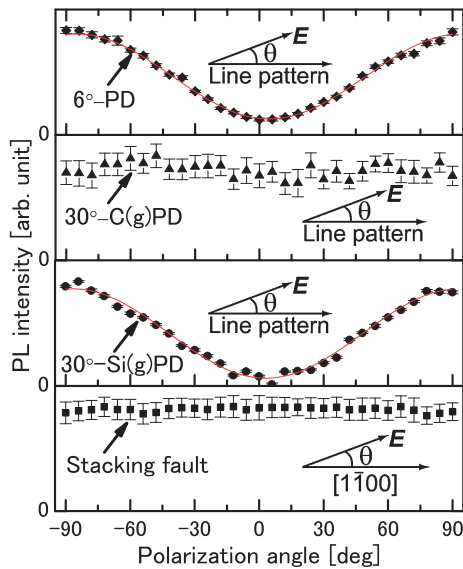
Fig. 3. Polarization of PL from the SSF, 30°-Si(g), 30°-C(g), and 6°-PDs. The horizontal axis indicates the angle of the electrical field of luminescence to [1$\bar{1}$00] for SSF, and to the line directions of the respective PDs. The red curves are sinusoids fitted to the PL intensity of the 30°-Si(g) and 6°-PDs.

study suggests that the luminescence originates from some dislocation centers of intrinsic nature binding carriers with an anisotropic wave function.

In contrast to 30°-Si(g) and 6°-PD segments, we found that the PL from 30-°C(g) PDs is not polarized as shown in Fig. 3. Another fact notable in Fig. 2(d) is that the PL from 30-°C(g) PDs is not uniform but is interrupted at places on the dislocation lines. One might explain these two facts by assuming that the luminescence originates in impurities precipitated along dislocation lines after the SSF expansion. Eberlein et al. reported a theoretical calculation on pinning of C(g) PDs by substituting atoms in the dislocation core with nitrogen atoms and the associated energy level in the band gap.[24] However, if we consider the precipitation of nitrogens along fresh dislocations, we need some mechanism for the enhanced diffusion of nitrogen atoms at room temperature in 4H-SiC, which has not been reported. An alternative explanation is that the luminescence originates from intrinsic defects on the PDs that have bound carriers with an isotropic wave function. The nonuniform PL from 30-°C(g) PDs may be explained by assuming nonradiative recombination centers distributed on the PDs.

We performed the PL mapping to expand the SSFs and PL imaging to investigate the polarization of PL from PDs bounding the SSFs. The PL from 6°-PDs tilted clockwise by 6° from the Peierls potential valley of screw dislocations was observed in addition to the well-known 30°-Si(g) and 30-°C(g) PDs in the same spectral region of luminescence from 30°-Si(g) PDs. We found that the PLs from the mobile 30°-Si(g) and 6°-PDs under illumination are polarized perpendicularly to their dislocation lines. In contrast, the PL from the immobile 30°-C(g) PDs is not polarized. This difference suggests that the carriers bound to the 30°-Si(g) and 6°-PDs have anisotropic wave functions and those bound to 30°-C(g) PDs have isotropic wave functions.

1) J. P. Bergman, H. Lendenmann, P. Å. Nilsson, U. Lindefelt, and P. Skytt: Mater. Sci. Forum **353–356** (2001) 299.
2) H. Lendenmann, F. Dahlquist, N. Johansson, R. Söderholm, P. Å. Nilsson, J. P. Bergman, and P. Skytt: Mater. Sci. Forum **353–356** (2001) 727.
3) H. Jacobson, J. Birch, R. Yakimova, M. Syväjärvi, J. P. Bergman, A. Ellison, T. Tuomi, and E. Janzén: J. Appl. Phys. **91** (2002) 6354.
4) S. Ha, M. Benamara, M. Skowronski, and H. Lendenmann: Appl. Phys. Lett. **83** (2003) 4957.
5) M. Skowronski, J. Q. Liu, W. M. Vetter, M. Dudley, C. Hallin, and H. Lendenmann: J. Appl. Phys. **92** (2002) 4699.
6) R. Hirano, Y. Sato, H. Tsuchida, M. Tajima, K. M. Itoh, and K. Maeda: Appl. Phys. Express **5** (2012) 091302.
7) A. Galeckas, J. Linnros, and P. Pirouz: Phys. Rev. Lett. **96** (2006) 025502.
8) A. Galeckas, J. Linnros, and P. Pirouz: Appl. Phys. Lett. **81** (2002) 883.
9) A. O. Konstantinov and H. Bleichner: Appl. Phys. Lett. **71** (1997) 3700.
10) K. X. Liu, R. E. Stahlbush, S. I. Maximenko, and J. D. Caldwell: Appl. Phys. Lett. **90** (2007) 153503.
11) M. Suezawa, Y. Sasaki, Y. Nishina, and K. Sumino: Jpn. J. Appl. Phys. **20** (1981) L537.
12) E. Depraetere, D. Vignaud, and J. L. Farvacque: Solid State Commun. **64** (1987) 1465.
13) I. Kiflawi and A. R. Lang: Philos. Mag. **30** (1974) 219.
14) N. Yamamoto, J. C. H. Spence, and D. Fathy: Philos. Mag. B **49** (1984) 609.
15) H. Sugimoto and M. Tajima: Jpn. J. Appl. Phys. **46** (2007) L339.
16) M. P. Peloso, B. Hoex, and A. G. Aberle: Appl. Phys. Lett. **98** (2011) 171914.
17) M. Tajima, E. Higashi, T. Hayashi, H. Kinoshita, and H. Shiomi: Mater. Sci. Forum **527–529** (2006) 711.
18) H. Jacobson, J. P. Bergman, C. Hallin, E. Janzén, T. Tuomi, and H. Lendenmann: J. Appl. Phys. **95** (2004) 1485.
19) P. Pirouz and J. L. Demenet: Philos. Mag. A **81** (2001) 1207.
20) S. I. Maximenko and T. S. Sudarshan: J. Appl. Phys. **97** (2005) 074501.
21) N. A. Mahadik, R. E. Stahlbush, J. D. Caldwell, and K. D. Hobart: Mater. Sci. Forum **717–720** (2012) 391.
22) Y. Ohno, I. Yonenaga, K. Miyao, K. Maeda, and H. Tsuchida: Appl. Phys. Lett. **101** (2012) 042102.
23) M. A. Razumova and V. N. Khotyaintsev: Phys. Status Solidi B **174** (1992) 165.
24) T. A. G. Eberlein, R. Jones, A. T. Blumenau, S. Öberg, and P. R. Briddon: Phys. Status Solidi C **4** (2007) 2923.